

Selective Spectral Detection of Continuum Terahertz Radiation

P. Kaufmann^{a,b}, R. Marcon^{c,d}, A. Marun^e, A.S. Kudaka^a, E. Bortolucci^b, M. Beny Zakia^b, J.A. Diniz^b, M.M. Cassiano^a, P. Pereyra^e, R. Godoy^e, A.V. Timofeevsky^f, V.A. Nikolaev^f, A. M. Pereira Alves da Silva^b, L.O.T. Fernandes^a

^a CRAAM – Escola de Engenharia, Universidade Presbiteriana Mackenzie, São Paulo, Brazil.

^b CCS – Universidade Estadual de Campinas, Campinas, SP, Brazil.

^c Instituto de Física “Gleb Wataghin”, Universidade Estadual de Campinas, Campinas, SP, Brazil.

^d Observatório Solar “Bernard Lyot”, Campinas, SP, Brazil.

^e Complejo Astronómico El Leoncito, CONICET, San Juan, Argentina

^f Tydex J.S. Co, St. Petersburg, Russia

ABSTRACT

The knowledge of THz continuum spectra is essential to investigate the emission mechanisms by high energy particle acceleration processes. Technical challenges appear for obtaining selective spectral sensing in the far infrared range to diagnose radiation produced by solar flare burst emissions measured from space as well as radiation produced by high energy electrons in laboratory accelerators. Efforts are being carried out intended for the development of solar flare high cadence radiometers at two THz frequencies to operate outside the terrestrial atmosphere (i.e. at 3 and 7 THz). One essential requirement is the efficient suppression of radiation in the visible and near infrared. Experimental setups have been assembled for testing (a) THz transmission of “low-pass” filters: rough surface mirrors; membranes Zitex G110G and TydexBlack; (b) a fabricated 2.4 THz resonant grid band-pass filter transmission response for polarization and angle of incidence; (c) radiation response from distinct detectors: adapted commercial microbolometer array using HRFZ-Si window, pyroelectric module and Golay cell; qualitative detection of solar radiation at a sub-THz frequency has been tested with a microbolometer array placed at the focus of the 1.5 m reflector for submillimeter waves (SST) at El Leoncito, Argentina Andes.

Keywords: THz radiometers, THz low-pass filters, THz sensors, Solar THz radiation

1. INTRODUCTION

Technologies for photometry and imaging in the THz range (arbitrarily 0.1 – 30 THz) are in full expansion for a variety of new and unique applications in different civil and military areas presenting a number of distinctive advantages on the well known microwaves or mid- to near-infrared technologies. THz radiation propagates well through cloth, dust and fog^{1,2,3}. Sensing in this range is proving to be particularly useful to determine internal characteristics of materials, in the search for drugs, mines and explosive materials. New biological and medical THz imaging applications are far reaching. Aerospace THz remote sensing applications include new approaches to determine atmospheric inhomogeneities and cloud characteristics^{4,5,6}.

Photometry and imaging at THz frequencies have important application in the diagnostics of radiation produced by high energy electrons, observed in laboratory accelerators⁷ as well as by thermal and non-thermal space plasmas^{8,9}. Solar flare accelerates electrons to high energies. Their radiation by synchrotron mechanism predicts intense fluxes in the far IR or THz range of frequencies¹⁰. We are currently characterizing materials and subsystems needed to assemble THz radiometers to be used in solar flare observations at discrete frequencies from the ground through the atmosphere 0.4 THz “window” at a high altitude site, and from space at 3 THz and 7 THz. One essential requirement to perform these measurements is the effective suppression of incoming visible and near infra-red (NIR) radiation. This can be obtained using a number of THz low-pass filters¹¹. We present the experimental developments of low-pass filters using rough surface mirrors^{12,13,14} and commercially available membranes: Zitex G110 G¹⁵ and TydexBlack¹⁶. A new set of resonant

mesh band-pass filters were fabricated to be tested for radiation polarization and angle of incidence. We studied the black body THz radiation comparative response of sensors: microbolometer array, pyroelectric module and Golay cell. Qualitative detection of solar radiation at a sub-THz frequency, 0.4 THz, has been verified with a microbolometer array placed at the primary focus of the 1.5 m reflector for submillimeter waves (SST) at El Leoncito, Argentina Andes.

2. THz LOW-PASS FILTERS

The radiometry of temperature enhancements above a pre-existent bright level – as it is the case of detection flare radiation excess over the solar disk intense emission – requires the effective suppression of all visible and NIR radiation. This was accomplished with the use of low-pass filters, summarized as follows.

2.1 Rough surface mirrors

The concept of roughened surface reflectors to diffuse visible and near infrared (NIR) radiation¹² has been considered for the first time for the photometer originally proposed for the SOHO mission¹³, later adopted for the Flare InfraRed Experiment (FIRE) proposal to the French-Brazilian Microsatellite mission¹⁷. Although these proposals were not accomplished, the concept has been validated at NASA/GSFC by the co-investigators of both proposals¹⁷. In order to confirm those early results, glass mirrors were fabricated and tested for reflectivity¹⁴. The results are illustrated in Fig. 1.

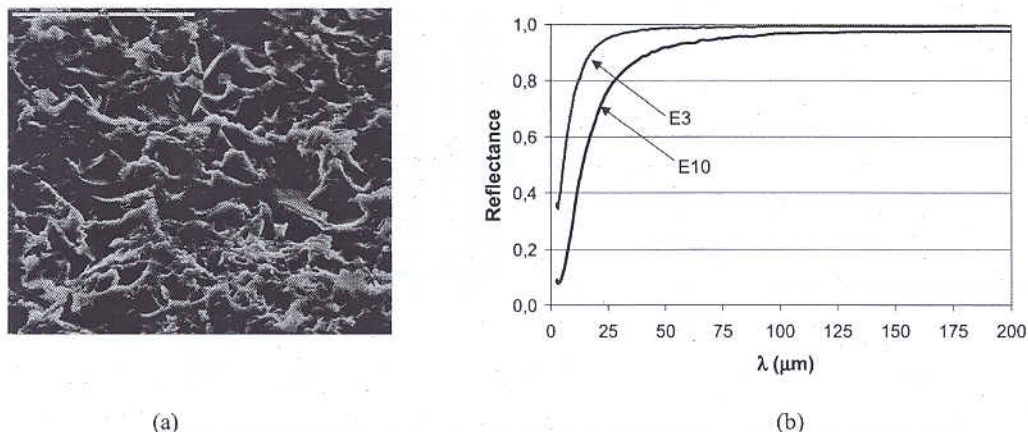


Fig. 1 (a) Electron micrograph of glass surface roughened with 10 μm Carborundum particles, E(10). A 50 μm scale is shown at the top. (b) Reflectance at 60° incidence angle measured at MPE, Garching, Germany, for E10, and for another glass surface roughened with 3 μm diamond particles (E3). They fit well 0.45 and 1.25 μm r.m.s. rough surfaces theory prediction, respectively^{12,14}.

2.2 The THz low-pass filter membranes

The membrane THz low-pass filters performance were recently evaluated¹¹. The Zitex G110 film (0.25 mm thickness, sintered Teflon with 1-2 μm pore sizes) is known as an effective suppressor of radiation with wavelengths shorter than 15 μm¹⁵. The results of measurements made at Tydex Company, at St. Petersburg, Russia, are shown in Fig. 2 (a) and (b). Although confirming the Zitex G110 transmittance in the THz range, careful inspection in the visible-near infrared range (< 15 μm) revealed a small amount of power transmission, corresponding approximately to about 0.3 % of the power in the visible-NIR. This amount may become significant in relative power since blackbody radiation at temperatures ranging 300-1000 K produce nearly 20 times more power in the visible-NIR compared to the power in the > 15 μm range.

Another membrane THz low-pass filter considered was the TydexBlack, produced by Tydex company¹⁶. The THz transmittance is shown in Fig. 3. The visible - near infrared transmittance of TydexBlack, shown in Fig. 3(b) is

considerably smaller compared to Zitex G110 (Fig. 2(b)). The power transmission in the NIR is $\ll 0.05\%$ (compared to the 0.2% measured for Zitex G110).

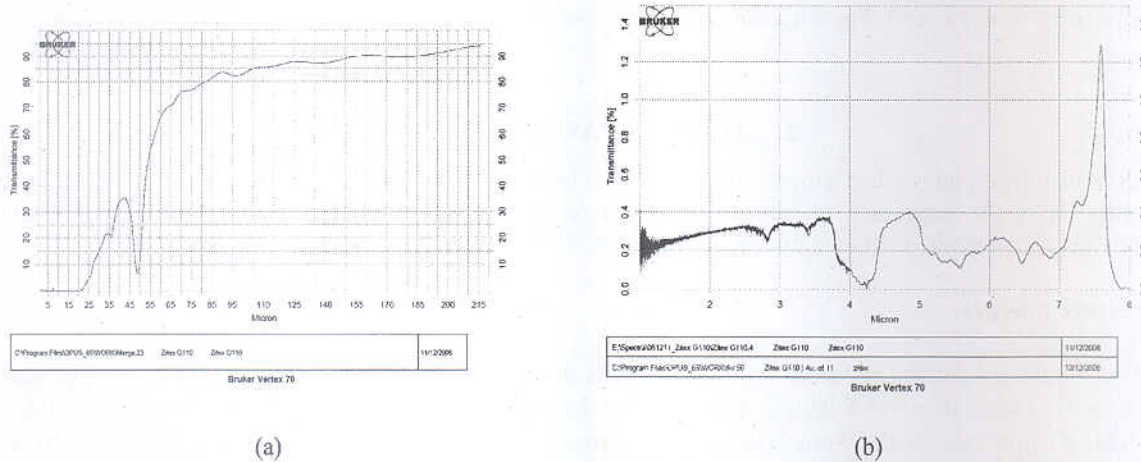


Fig. 2 – The Zitex G110 visible-THz transmission in (a), measured in detail for the visible and NIR in (b)

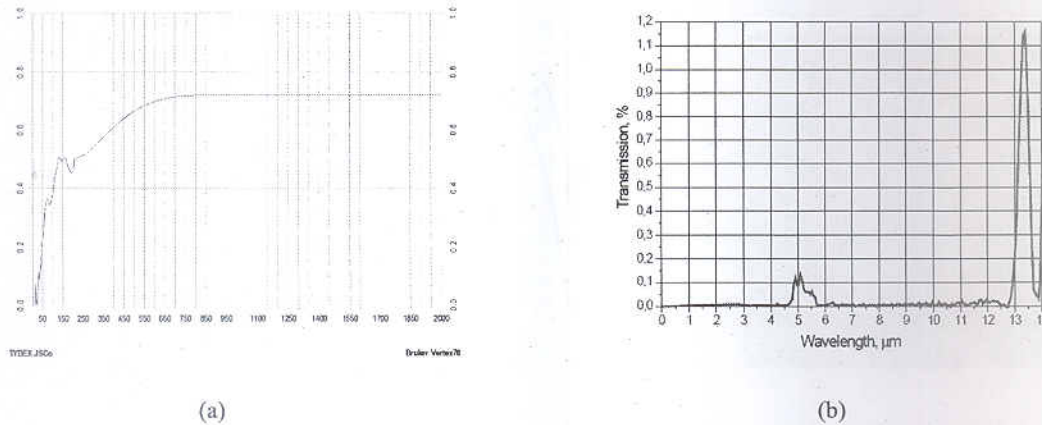


Fig. 3 Transmittance of TydexBlack in THz range (a) and in the visible-NIR (b)

Inspecting the results shown in Figs. 2 and 3 it can be concluded that the complete suppression of visible-NIR can be obtained with a sandwich of membranes Zitex G110 with TydexBlack, for applications in the ≤ 7 THz frequencies.

3. RESONANT BAND-PASS METAL MESH FILTER TRANSMISSION

A new set of resonant metal mesh band-pass filters tuned at 2.4 THz were fabricated for transmission tests, holding the filter on THz “transparent” material, under different angles of incidence and radiation polarization. The basic technique for the filters fabrication was described elsewhere¹⁸. The mesh thickness control was accomplished by adding successive layers of metal deposition. Fig. 4 shows the transmission simulation for the 2.4 THz ($\pm 10\%$ band pass) constructing parameters in (a) and electron micrographs of the fabricated filter in (b). The mesh thickness was of about 7 μm .

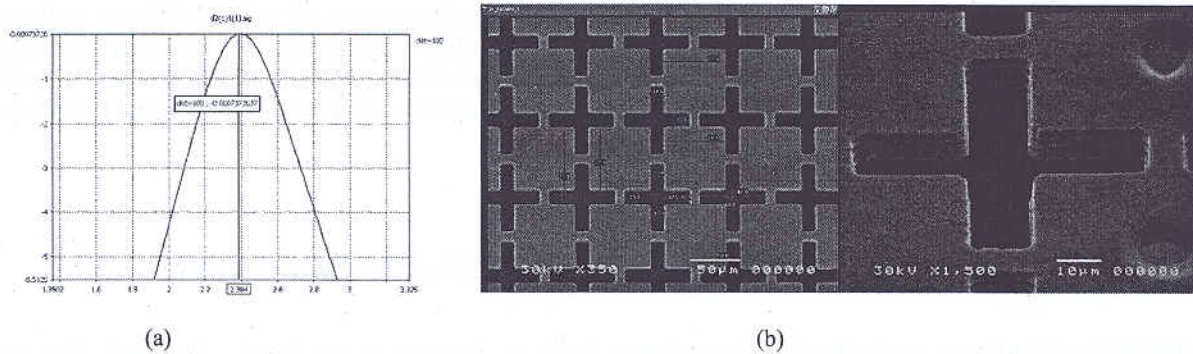


Fig. 4 – Resonant metal mesh band-pass filter designed for 2.4 THz. Simulated transmission performance is shown in (a). Fabricated mesh electron micrographs in (b).

The transmission was measured for the suspended metal mesh, for the applied on a TPX base, and for sandwiches of mesh plus TPX and TydexBlack, performed at Tydex Company. The results are shown in Fig. 5. The central frequency and band-pass agrees with the simulated design, based on the parameters set for fabrication, which are close to the actually measured parameters (see Fig. 4).

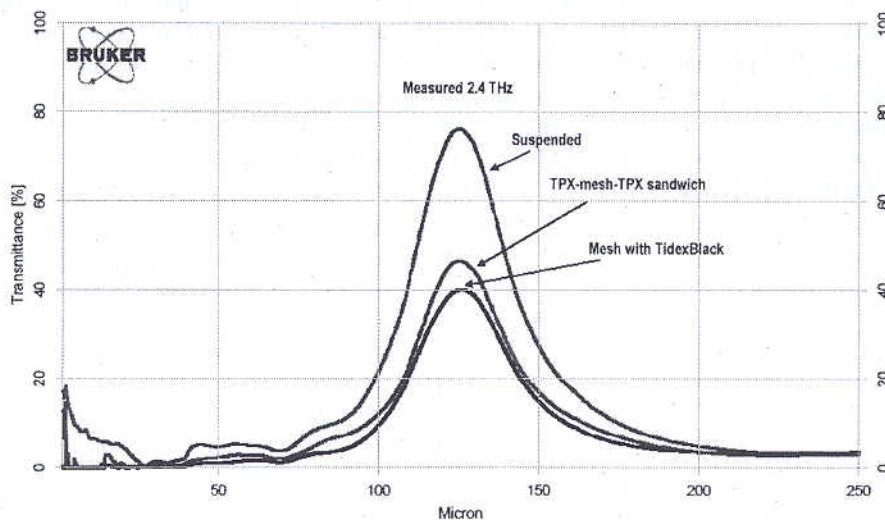


Fig. 5 – Measured transmission of the metal mesh filter designed (Fig. 4), suspended free, and in sandwich with TPX and with TydexBlack THz low-pass filter.

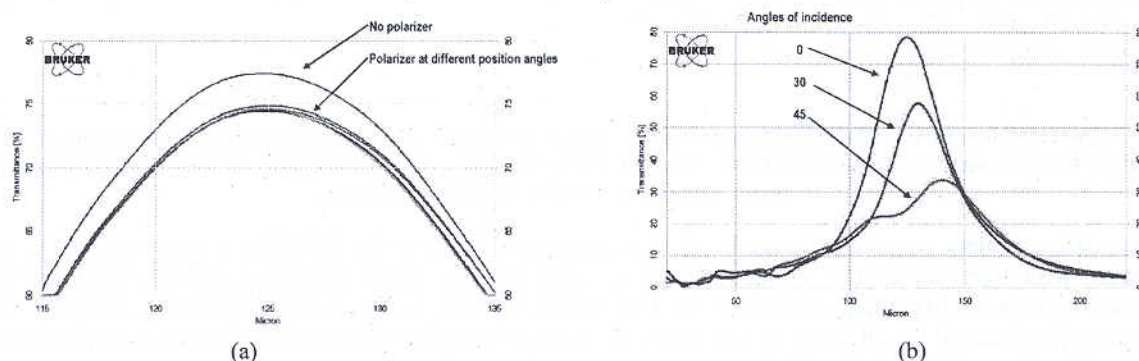


Fig. 6 - 2.4 THz mesh band-pass filter transmission for polarized radiation in (a). Plots overlap for position angles 0° , 30° , 60° , and 90° . (b) Transmission for angles of incidence of incoming radiation (in degrees).

The 2.7 THz metal mesh filter has been also tested for transmission of incoming radiation at different polarization angles, as well for different angles of incidence. The results are shown in Fig. 6 (a) and (b). The filter transmission is the same independently from the polarization position angle. The dependence on the angle of incidence, however, becomes important for angles larger than about 20° . These effects are more pronounced compared to similar metal mesh 2.2 THz filters fabricated on $3.8 \mu\text{m}$ polyester substrate¹⁹.

4. EVALUATION OF UNCOOLED SENSORS FOR THZ RADIATION

The qualitative performance evaluation for three distinct kinds of detectors is now briefly described. The sensors evaluated consisted in one adapted microbolometer array camera; a piroelectric module and one optocoustic detector (Golay cell).

4.1 – Adapted microbolometer array camera

A custom-made detector consisted in a room-temperature vanadium oxide micro-bolometer focal plane array (FPA) camera IRM 160 A with HRFZ-Si THz window provided by INO Company, Quebec, Canada²⁰. The camera total-power response for black body temperatures ranging 300-1000 K was measured at El Leoncito laboratory. A nichrome resistor, assumed as close to an ideal black body radiator, was placed at the focus of 150 mm concave reflector to produce an image occupying nearly 70 % of the FPA. We selected the Region Of Interest (ROI) over the area in the frame filled by the heated resistor image. All pixels readings on the ROI were added and averaged for every frame reading, quoted in camera reading units. Several sets of measurements were taken, for temperatures ranging from ambient (about 290 K) to about 900 K, without any low-pass filter, and using the two membrane low-pass filters described in Section 2.2. One series of measurements are summarized in Fig. 7 (a). Figure 7(b) shows another expanded set of data showing the camera response using the Zytex G110 (in (a) and (b) and the TydexBlack low-pass membranes in (b).

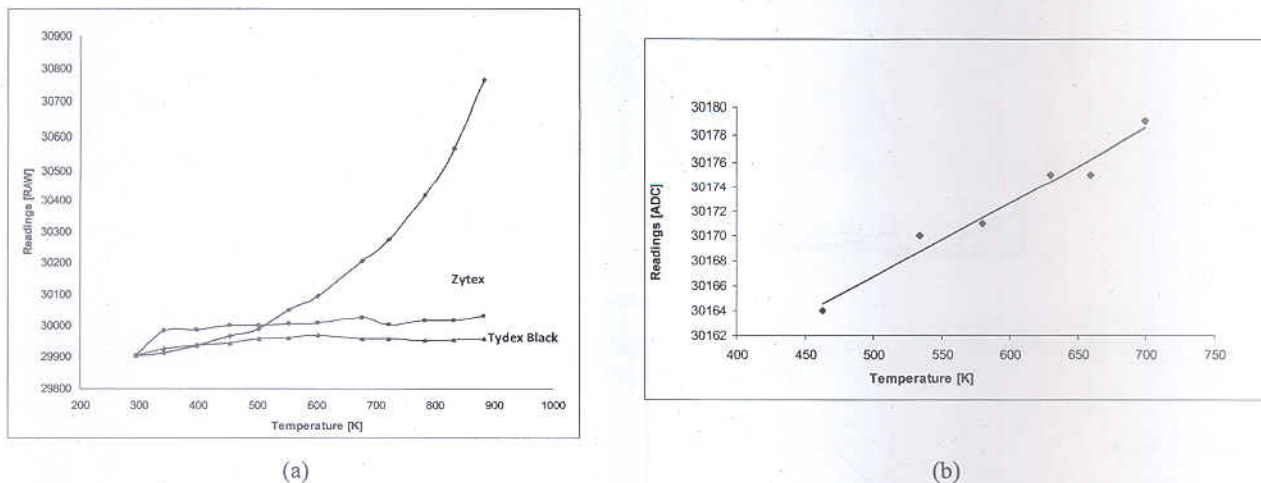


Fig. 7 - The response of INO IRM 160A camera FPA with HRFZ-Si window to black body radiation, for the whole spectrum and through the low-pass membranes: (a) filters for the THz spectral contribution., (b) expanded plots for TydexBlack low-pass filter. The output ordinates are in ADC camera reading units.

The fluctuation of data points can be attributed to measurement uncertainties (of about ± 1 reading units), since they were taken with high cadence (30 frames/s). It can be noted that the camera readings with Zytex G110 low pass filter interposed is about 20-40 reading units above the TydexBlack readings, for the whole range of temperatures. This effect was repeatedly observed for all series of measurements. It might correspond to the fraction of power in the visible-NIR transmitted by Zytex G110 (see Fig. 2(b)).

The substantial reduction in the camera response to black body temperature changes when interposing the low-pass membranes proves their effectiveness in suppressing the visible and NIR radiation. Indeed the predicted ratio of power increase for a black body heated about 100 K, at the 700 K level, for the whole main spectrum ($\lambda > 0.5 \mu\text{m}$) in comparison to the THz part of the spectrum ($\lambda > 15 \mu\text{m}$) is close to 60. This might be compared to ratio of about 40 between the camera ROI readings increase in that range (about 150 units) compared to the readings increase with the membrane low-pass filters (about 4).

The camera scale of about 25 K per reading unit (± 1 reading unit) was too large to allow any measurable differences when adding one resonant metal mesh band-pass filter. However we placed the camera + low-pass filter + 0.4 THz band-pass filter assembly at the Newtonian focus of the 1.5-m SST reflector²¹ to obtain a stronger incoming signal (see Fig. 8).

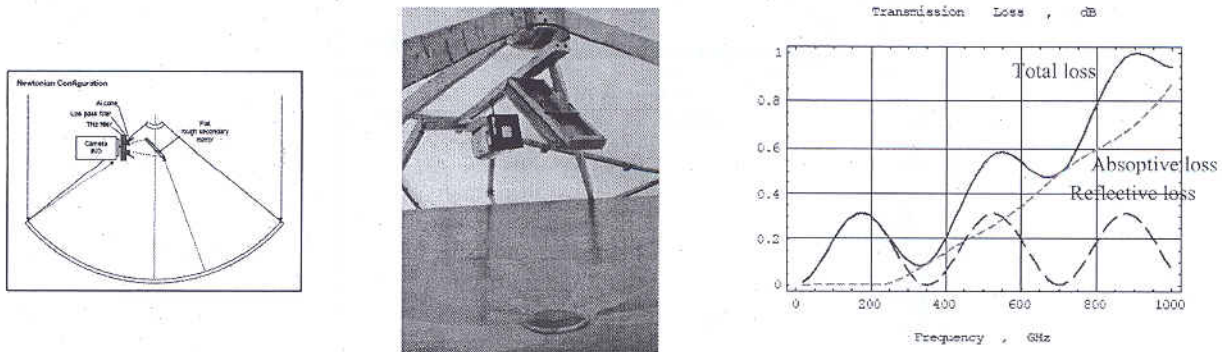


Fig. 8 – The INO camera, with low-pass membrane and band-pass metal mesh filter installation at the Newtonian focus of the SST 1.5-m reflector²¹. The secondary mirror has a glass roughened flat surface to further diffuse the thermal and visible radiation. The plot at right shows the GoreTex radome transmission loss²², that becomes pronounced for frequencies > 0.6 THz.

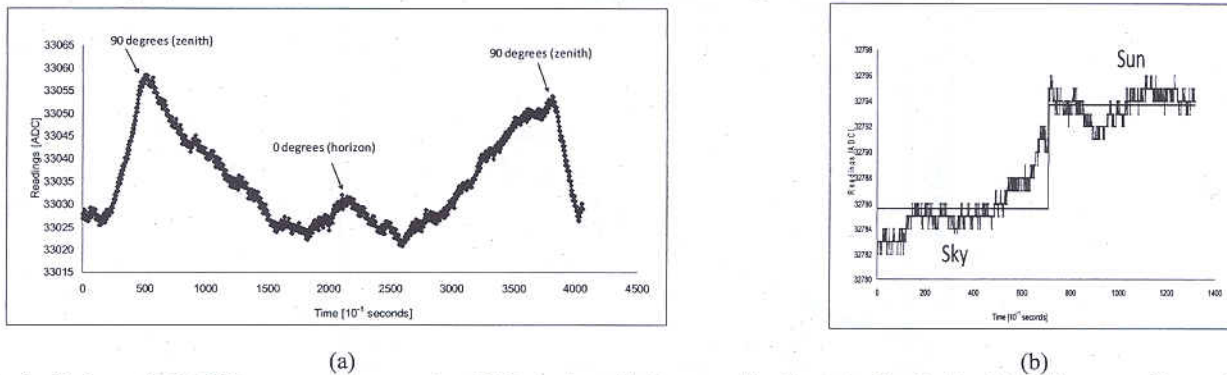


Fig. 9 – Bolometric 0.4 THz measurements made at El Leoncito with the assembly shown in Fig. 8: (a) with ordinates reading scale decreases for temperature increases, the sky temperature with elevation angle, from zenith to horizon. The small decrease at zero elevation angle is due to cooler snowy mountains in the horizon. (b) One example of on-off solar observation.

Successful detection of sky temperature variations with elevation angle and of solar radiation at 0.4 THz has been obtained, illustrated in Fig. 9. (a) Sky temperature difference from zenith to horizon (of about 110 K) is consistent with attenuation of $\tau = 1.0$ neper, typical at 0.4 THz at El Leoncito site. (b) The on-off solar observation (with the Sun at 30 deg elevation): 33 K, corresponds to 264 K, corrected for atmosphere attenuation. This result indicate a poor beam efficiency ($264/5000 = 0.05$), that may be due to incomplete optical alignment of the camera FPA.

4.2 - Pyroelectric detector module

The pyroelectric modular detector made by Spectrum Detector Inc.²³, model SPH65-THz, was tested at the laboratory of the Center for Semiconductor Components (CCS), State University of Campinas. The setup utilised a standard laboratory Newport model 67030 black body source with a build-in wheel chopper, set at 20 Hz. The detector response

to black body temperatures is shown in Fig. 10 for open conditions (responding to the visible – THz range), and for low-pass membranes interposed.

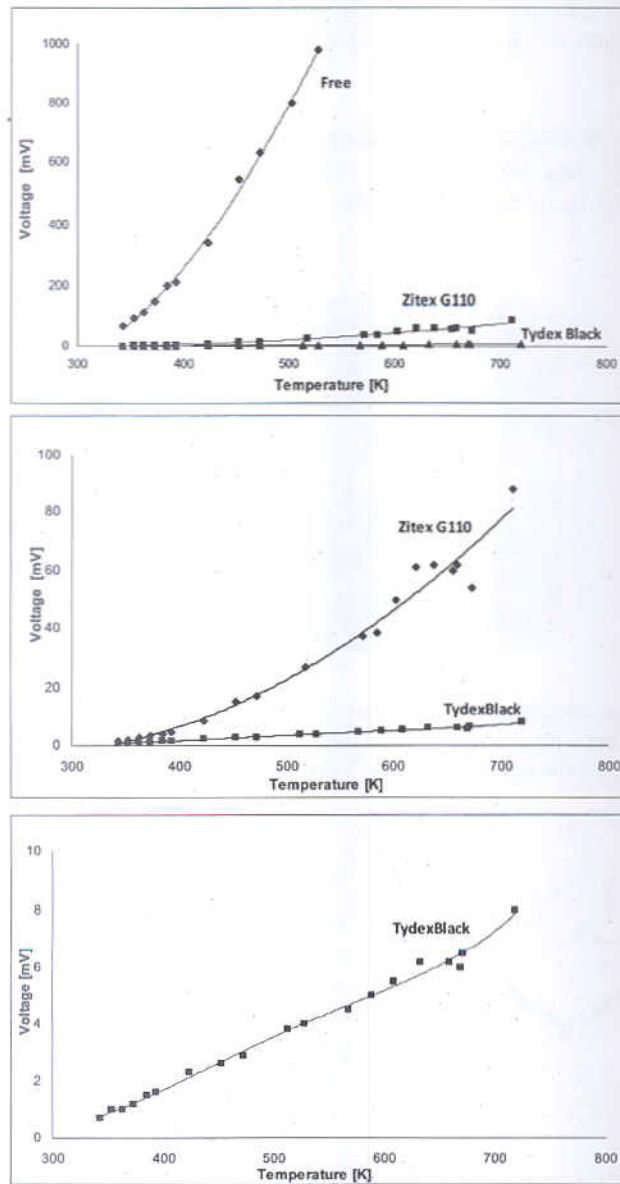


Fig. 10 – The Spectrum Detector SPH65-THz pyroelectric module peak-to-peak mV response to black body temperatures, for open conditions, and with low-pass membrane filters interposed: Zitex G110 and TydexBlack. Chopper frequency was 20 Hz

The pyroelectric response to blackbody temperature variations was considerably better defined, compared to the microbolometer array response as described in Section 4.1. The detector readings with Zitex G110 low pass filter are larger than the readings with TydexBlack, increasing with temperatures (see middle panel in Fig. 10). This effect might correspond to the fraction of power in the visible-NIR transmitted by Zitex G110 (see Fig. 2(b)). The small proportion of power allowed through with the use of the low-pass filter is consistent with the efficient suppression of visible and NIR radiation. Transmission tests were performed by adding a 2 THz metal mesh band-pass filter. For higher temperatures there were indications on power reduction, qualitatively consistent with the expected band-pass. The measured output, however, was close to the output reading fluctuations, preventing the reliable reading of several data points, for different temperatures.

4.3 – THz performance of the opto-acoustic Golay cell detector

The performance of the Tydex model GC-1P Golay cell sensor²⁴ was investigated on similar conditions. The first set of measurements was carried out at Tydex Company, using a standard black body, 2 mm diameter aperture and a wheel chopper. Filters and diaphragm were interposed in front of the Golay cell. We report here the measurements taken using a 2 mm diaphragm close to the detector, chopper frequency of 20 Hz.

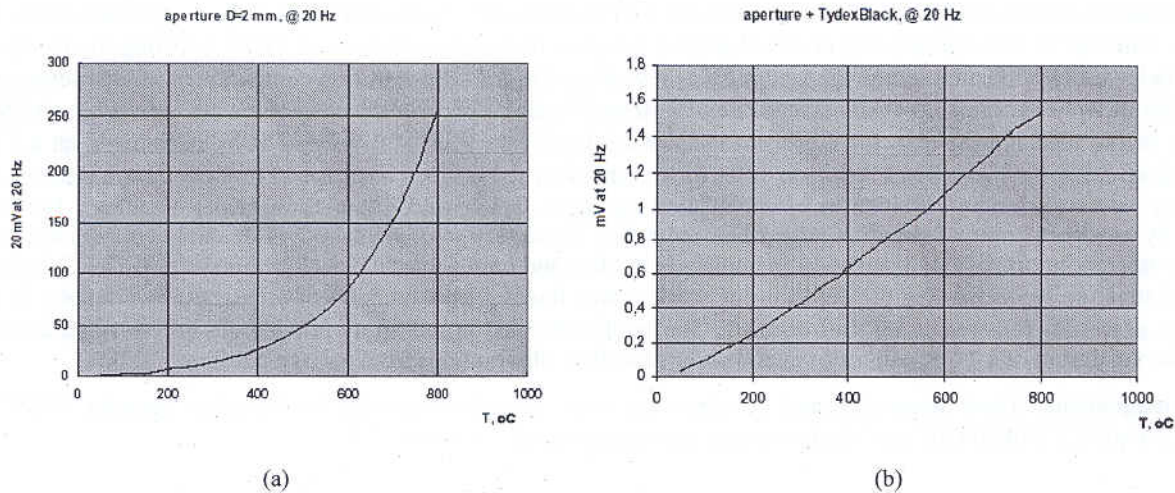


Fig. 11 – The Tydex GC-1P opto-acoustic detector (Golay cell) response to black body temperature variations. (a) No filter interposed. (b) TydexBlack low-pass filter interposed.

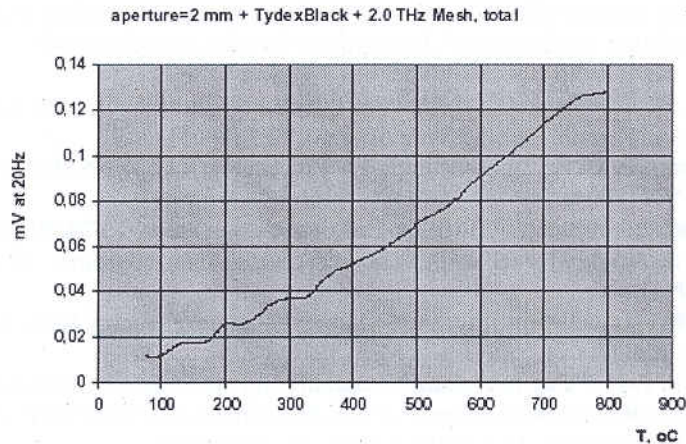


Fig 12 – The Tydex GC-1P Golay cell response to black body temperature variations with low-pass filter TydexBlack and 2 THz metal mesh band-pass filter interposed

A 2 THz band-pass resonant metal mesh filter was added to the low-pass membrane filter, producing the nearly linear response shown in Fig. 12. The reduction in detector outputs for low-pass filter (frequencies < 6 THz) and for band-pass filter added (2 ± 0.2 THz) to the low-pass filter are consistent with the spectral power reduction in the respective band. The sensitivity of the Golay cell can be further increased with the use of the input photon collecting cone and/of by adding a small reflecting aperture.

5. CONCLUDING REMARKS

We describe the performance of materials and detectors needed for the construction of a THz radiometer applied to solar flare observations outside the terrestrial atmosphere. They included low-pass membrane filters, metal mesh resonant band-pass filter and sensors. The observation of small temperature enhancements above one intense source such as the Sun requires the effective suppression of all visible and near radiation that dominates the blackbody spectrum in the 10^3 K range. This can be accomplished by combining three low-pass filters (frequencies < 6 THz): diffusing the incoming thermal radiation by reflection in a roughened mirror preventing it to heat the detection compartment of the radiometer; a sandwich of two membrane low-pass filters Zitex G110 and TydexBlack to completely attenuate the visible and NIR radiation before reaching the detector. Resonant metal mesh band-pass filter at 2.4 THz has been mounted on a TPX surface sandwich with TydexBlack low-pass filter for transmission tests. It has been found that the transmission is not dependent on the incoming radiation polarization position angle. Transmission and filter center frequency becomes affected by incidence angle of radiation larger than about 20° . The detection of black body THz radiation from has been tested for microbolometer focal plane array, pyroelectric module and opto-acoustic detector (Golay cell). The Golay cell exhibited superior sensitivity for the detection of weak power fraction as a function of temperature variations in the band-pass of $\pm 10\%$ centered at a THz frequency. The results obtained in this study provide the necessary parameters needed for the design of a THz radiometer intended for solar flare observations from a space platform.

Acknowledgements. These researches and developments were partially supported by Brazilian agencies FAPESP, CNPq, CNPq/INCT-NAMITEC and Mackpesquisa, and Argentina agency CONICET.

REFERENCES

- [1] Harris, D.C., "Materials for infrared windows and domes", SPIE Optical Engineering Press, Washington, USA (1999).
- [2] Siegel P. H., "THz Technology: An Overview", International Journal of High Speed Electronics and Systems, **13**, n^o2, 1-44 (2003).
- [3] Mlynczak, M., Johnson, D., Bingham, G., *et al.*, "Far-Infrared Spectroscopy of the Troposphere (FIRST) project", Proceedings of Geoscience and Remote Sensing Symposium, **1**, 512 (2003).
- [4] Sherwin M. S., Schmuttenmaer C. A., Bucksbaum P. H., Proceedings of DOE-NSF-NIH Workshop on Opportunities in THz Science, Arlington, VA (2004).
- [5] Kinch, M.A., "Infrared detector materials", SPIE Optical Engineering Press, **TT76**, Washington, USA, DC (2007).
- [6] Strabala K. I., Ackerman S. A. and Menzel W. P., "Cloud Properties inferred from 8-12- μ m Data", *Journal of Applied Meteorology*, **33**, 2, 212 (1994).
- [7] Williams, G. P., "FAR-IR/THz radiation from the Jefferson Laboratory, energy recovered linac, free electron laser", *Rev. Sci. Instrum.* **73**, 1461-1463 (2002).
- [8] Kaufmann, P. and Raulin, J.-P., "Can microbunch instability on solar flare accelerated electron beams account for bright broadband coherent synchrotron microwaves?", *Phys. Plasmas* **13**, 070701-070701-4 (2006).
- [9] Klopf, J. M., in *1st SMESE Workshop*, 10-12 March, Paris, France (2008).
- [10] Kaufmann, P. *et al.*, *Astrophys. J.*, **603**, L121 (2004).
- [11] Kaufmann, P. *et al.*, "Continuum Terahertz Radiation Detection Using Membrane Filters", International Microwave and Optoelectronics Conference, SBMO & IEEE-MTT, Nov. 3-6 2009, Belem, Pará, Brazil, 262-266 (2009).
- [12] Bennett, H.E. and Porteus, J. O. "Relation between surface roughness and specular reflectance at normal incidence", *J. Opt. Soc. Am.* **51**, 123-129 (1961).
- [13] Kostiuk.T. and Deming, D., "A solar infrared photometer for space flight application", *Infrared Physics* **32**, 225-233 (1991).
- [14] Kornberg, M. *et al.*, "Rough Mirrors for the THz Frequency Range", Proc. MOMAG 2008 - 13th SBMO and 8th CBMAG, Florianópolis, SC, Brazil, 7-10 September 2008, 365-367 (2008).

- ^[15] Benford, D.J., Gaidis, M.C., and Kooi, J.W., "Optical properties of Zitex in the infrared to submillimeter", *Applied Optics* **42**, 5118-5122 (2003).
- ^[16] www.tydex.ru, Tydex JSCo, St. Petersburg, Russia, Technical Note on THz materials and components (2008).
- ^[17] Kaufmann, P. *et al.*, "Flare InfraRed Experiment (FIRE)", NASA proposal to FBMS in response to AO-98-OSS-01 (1998).
- ^[18] Melo, A.M. *et al.*, "Metal mesh resonant filters for terahertz frequencies", *Applied Optics* **47**, 6064-6069 (2008)
- ^[19] MacDonald, M.E. *et al.*, "Spectral transmittance of lossy printed resonant-grid terahertz bandpass filters", *IEEE Trans. on Microwave Theory and Techniques* **48**, 712-718 (2000).
- ^[20] <http://www.ino.ca/en-CA>
- ^[21] Kaufmann, P. *et al.*, "New telescopes for ground-based solar observations at submillimeter and mid-infrared", in Ground-based and airborne telescopes II (ed. By L.M. Stepp and R. Gimozzi), *Proc. SPIE* **7012**, 70120L-1-70120L-8 (2008)
- ^[22] ESSCO, West Concord, MA, USA, private communication (2008).
- ^[23] <http://www.spectrumdetector.com>
- ^[24] http://www.tydexoptics.com/products1/thz_optics/golay_cell/